Effective light trapping in polycrystalline silicon thin-film solar cells by means of rear localized surface plasmons

Zi Ouyang,[1,a)] Supriya Pillai,[1] Fiona Beck,[2] Oliver Kunz,[1,b)] Sergey Varlamov,[1] Kylie R. Catchpole,[2] Patrick Campbell,[1] and Martin A. Green[1]
[1]*ARC Photovoltaics Centre of Excellence, The University of New South Wales, Sydney, New South Wales 2052, Australia*
[2]*Centre for Sustainable Energy Systems, Australian National University, Canberra, ACT 0200, Australia*

(Received 11 March 2010; accepted 14 June 2010; published online 1 July 2010)

Significant photocurrent enhancement has been achieved for evaporated solid-phase-crystallized polycrystalline silicon thin-film solar cells on glass, due to light trapping provided by Ag nanoparticles located on the rear silicon surface of the cells. This configuration takes advantage of the high scattering cross-section and coupling efficiency of rear-located particles formed *directly* on the optically dense silicon layer. We report short-circuit current enhancement of 29% due to Ag nanoparticles, increasing to 38% when combined with a detached back surface reflector. Compared to conventional light trapping schemes for these cells, this method achieves 1/3 higher short-circuit current. © *2010 American Institute of Physics*. [doi:10.1063/1.3460288]

Polycrystalline silicon (poly-Si) on glass is a promising emerging thin-film solar cell technology. It combines the advantages of silicon (Si) wafer-based technology with low material usage and large-area monolithic construction typical for the thin-film approach.[1] One of the most recent trends in the development of poly-Si thin-film cell technology is replacing the relatively slow and expensive plasma enhanced chemical vapor deposition (PECVD) of precursor amorphous Si (a-Si) diodes by the much faster, cheaper, and simpler electron-beam evaporation. Recently, efficiencies for evaporated poly-Si thin-film modules on planar glass have been demonstrated to be comparable to the performance of equivalent planar cells made by PECVD.[2,3] In order to further improve the cell efficiency, effective light trapping is required. Glass substrate texturing, the approach conventionally used for PECVD cells, has proven to be difficult to apply to evaporated cells due to the line-of-sight deposition that leads to defective Si microstructure on textured substrates.[4] Hence there is a need for alternative light-trapping approaches that do not rely on substrate texturing. The excitation of localized surface plasmons in metal nanoparticles is one such technique.

Scattering from plasmonic nanoparticles can couple a large fraction of incident light into trapped modes within a nearby semiconductor layer. The nanoparticle size, geometry, and material, as well as the local dielectric environment can be chosen in order to maximize the light scattering and coupling efficiency.[5] Performance enhancement for Si thin-film solar cells using plasmonic light trapping has been reported by several groups.[6–8] Typically the nanoparticles were formed on a thin dielectric layer in the front of Si thin-film cells, which was necessary for the Si surface passivation. However, recently it has been shown that locating the nanoparticles on the rear of a solar cell can avoid suppression at wavelengths below resonance caused by the interference effects, while still allowing effective coupling of the long wavelength light.[9] Additionally, previous numerical simulations have shown that the scattering cross-section of rear-located particles increases dramatically with decrease in thickness of the dielectric spacer layer between the Si surface and the particle layer, for the case where this layer is less than 10 nm thick.[10]

In this work, we present experimental results for two different configurations of nanoparticles, with and without the dielectric spacer layer. We show that nanoparticles formed *directly* on Si can enhance the short-circuit current of the cells by 29% due to light trapping, which is more than double the enhancement provided by the particles on a 30 nm thick SiO_2 spacer layer. A combination of the Ag nanoparticles *directly* on the Si surface with a detached back surface reflector (BSR) further improves the enhancement to 38%; a relative increase of 1/3 compared to the best previously reported BSR (Ref. 11) used for planar evaporated poly-Si thin-film cells.

The 2 μm thick a-Si precursor diode was deposited by electron-beam evaporation onto planar borosilicate glass. The cell structure is illustrated in Fig. 1(a). After deposition the films were crystallized, annealed, and hydrogen plasma passivated. The poly-Si diodes with 4×10^{15} cm^{-3} absorber

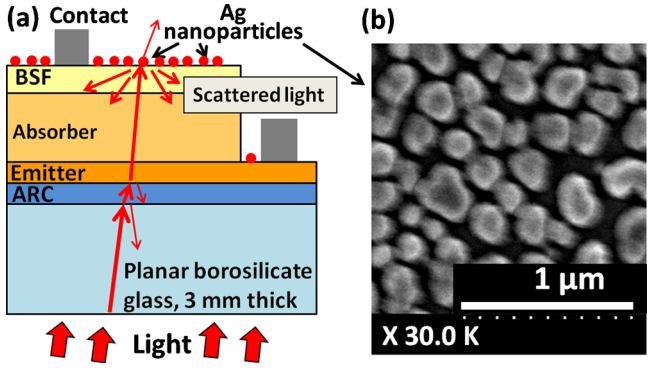

FIG. 1. (Color online) (a) Cross-sectional schematic of an evaporated solar cell in superstrate configuration. Ag nanoparticles are applied to the rear surface (not to scale). Note the light scattered back by the surface plasmons. (b) SEM image of a Ag nanoparticle coating on the poly-Si surface.

a)Electronic mail: ouyangzi@gmail.com.
b)Present address: CSG Solar Pty Ltd, 82 Bay Street, Botany New South Wales 2019, Australia.

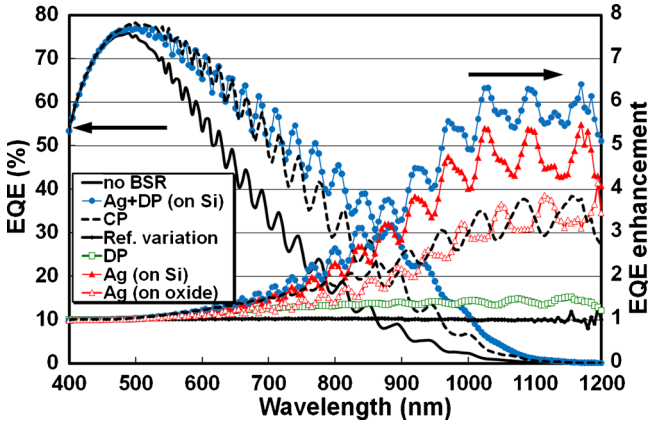

FIG. 2. (Color online) EQE (left axis) and EQE enhancement (right axis) of an evaporated cell with different light-trapping methods: Ag nanoparticles (Ag, red triangles), detached paint (DP, green squares), Ag nanoparticles plus DP (Ag+DP, blue circles), and contact paint (CP, dashed line). EQE variation in a reference sample is also provided (reference variation, black dots).

doping were then metallized to 2 cm^2 cells using interdigitated line contacts on both the emitter and the back surface field (BSF) layers. A reference sample underwent the same metallization.

The nanoparticles were formed by thermal evaporation of a Ag film *directly* onto the metallized rear Si cell surface followed by a 50 min anneal at 200 °C in N_2 atmosphere. Silver was selected because of its low parasitic light absorption and good scattering properties.[5] For comparison, we also fabricated Ag nanoparticles on equivalent cells but with a 30 nm SiO_2 spacer layer (on top of the rear cell surface, refractive index 1.6). The reference cell underwent the same processing steps but was masked during the Ag evaporation. Since a fraction of light still escapes the cells through the rear surface, the best performing Ag nanoparticles were combined with an additional detached reflector, composed of white acrylic indoor paint on a flexible substrate placed behind the cells (with a visible air gap). The best previously reported BSR for evaporated poly-Si thin-film cells is the same paint *directly* on the cell's rear surface.[11] For comparison, we also included this light-trapping scheme in our study.

External quantum efficiency (EQE) measurements, dark and light I-V measurements and scanning electron microscopic (SEM) imaging were performed to characterize the cells and the nanoparticles.

A SEM image of the Ag nanoparticles is shown in Fig. 1(b). The particle size is of the order of 150–250 nm with a particle coverage of ~50%.

EQE measures the ratio of collected (photogenerated) carriers to incident photons as a function of the wavelength. Figure 2 shows the EQE (left axis) and the EQE enhancement ($EQE_{light\text{-}trapping}$ divided by $EQE_{initial}$, right axis) measured on the same cell. Data is shown for the cell with nanoparticle *directly* on the Si (Ag on Si, red, solid triangles), with detached white paint (DP, green squares), with a combination of the two (Ag+DP on Si, blue circles), with contact paint (CP, dashed line), and with no BSR (black line), i.e., the initial condition. Data is also shown for a cell with 30 nm SiO_2 spacer layer between the Si and the nanoparticles (Ag on oxide, red, hollow triangles). All investigated light-trapping schemes enhanced the EQE at wavelengths longer than 450 nm. This is because light of wavelengths shorter than 450 nm is fully absorbed during its first pass through the 2 μm thick Si films. At 1100 nm, corresponding to approximately the band gap of Si, the EQE enhancement due to the nanoparticles *directly* on the Si surface is roughly 30% higher than that due to the nanoparticles on the oxide spacer layer. When the Ag nanoparticles formed *directly* on the Si surface are combined with a detached paint reflector, a sixfold EQE enhancement is observed at wavelengths around 1100 nm. In this configuration light that is not initially coupled back into the Si by the nanoparticles is reflected toward the cell by the detached reflector. This approach provided a significantly larger EQE enhancement in wavelengths above 600 nm, when compared with the contact white paint.

TABLE I. Light I-V characteristics of an evaporated cell with no BSR, detached paint (DP), Ag nanoparticles (Ag), and Ag combined with DP (Ag+DP). Percentages in the brackets are the enhancement compared to the case without a BSR on the same cell.

Sample condition	J_{SC} (mA/cm^2)	V_{OC} (mV)	*FF* (%)	*Eff* (%)
No BSR	14.5	404	64.7	3.79
DP	16.46 (14%)	412	64.3	4.36 (15%)
Ag	18.74 (29%)	408	60.9	4.66 (23%)
Ag+DP	19.99 (38%)	413	60	4.95 (31%)

The short-circuit current density (J_{sc}) can *directly* be calculated from the EQE data as follows:

$$J_{sc} = q \int \mathrm{EQE}(\lambda) S(\lambda) d\lambda,$$

where q is the electron charge and $S(\lambda)$ is the standard spectral photon density of sunlight at the earth's surface (Air Mass 1.5). According to this calculation, the J_{sc} enhancement is 29% for the case of nanoparticles *directly* on the Si surface and 16% for the nanoparticles on the oxide layer. When the Ag nanoparticles were combined with the detached paint, the enhancement increased up to 38% and 30%, respectively. The contact paint, which was the best performing BSR, provided 28% J_{sc} enhancement. This enhancement agrees with the value demonstrated in Ref. 2 and predicted by Ref. 11. It is clear that the highest J_{sc} enhancement among all the tested light-trapping approaches is provided by the combination of Ag nanoparticles (*directly* on the Si surface) and the detached paint, and is about 1/3 higher than the contact paint BSR.

It is also shown in Fig. 2 that the EQE variation in the reference sample before and after Ag nanoparticle fabrication was negligible. This indicates that the process steps necessary to fabricate the nanoparticles do not affect the cell performance and that the EQE characterization is reliable and repeatable.

The experimental light I-V parameters for the cells with and without Ag nanoparticles fabricated *directly* on the Si are shown in Table I. It can be noted that the Ag nanoparticles enhanced J_{sc} significantly while the open-circuit voltage remained nearly unchanged. The fill factor decreased with increasing J_{sc}, which is a result of larger parasitic series resistance losses and is mainly related to the preliminary metallization that was employed. Dark I-V characteristics did not show any evidence of shunting due to *direct* contact of the nanoparticles with the Si surface and the metal contacts.

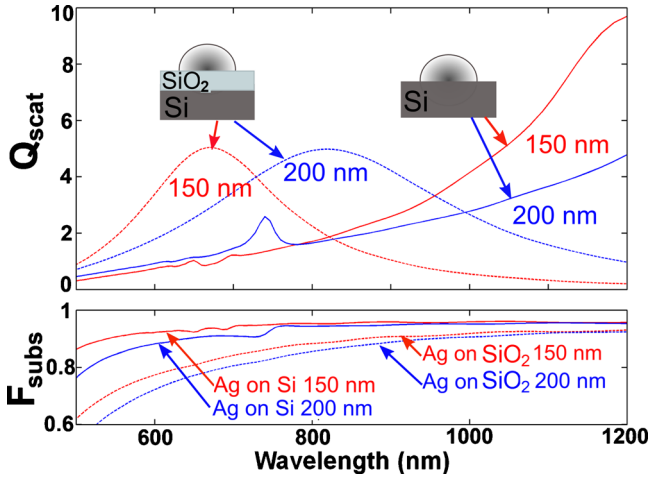

FIG. 3. (Color online) Calculated Q_{scat} spectra for single Ag nanoparticles (150 and 200 nm diameter) on Si substrates, located either *directly* on the Si (solid line) or on a 30 nm SiO_2 layer (dashed line). Inset shows F_{subs}.

As a result, the conversion efficiency increased significantly due to the existence of the Ag nanoparticles and the detached paint.

To compare the light trapping provided by Ag nanoparticles with and without a spacer layer, finite-difference time-domain (FDTD) numerical simulations were performed using the FDTD solutions package from Lumerical.[12] These simulations for the scattering behavior of nanoparticles have been shown to agree qualitatively with experimental results for random nanoparticle distributions.[9] In this work, the normalized scattering cross-section spectra (Q_{scat}) and the coupling efficiency (F_{subs}) were calculated for single hemispherical particles of diameter 150 and 200 nm located either *directly* on a semi-infinite Si substrate or separated from the Si by a 30 nm silicon oxide spacer layer. The particle diameters correspond to the median of the particle sizes seen experimentally. Q_{scat} can be thought of as the area over which the particle scatters light, normalized to the cross-sectional area of this particle. F_{subs} is defined as the fraction of light that is scattered and coupled into the Si. Details of the simulation setup can be found in Ref. 10.

Figure 3 shows Q_{scat} for Ag nanoparticles with diameters of 150 and 200 nm on a Si substrate. Data is shown for particles *directly* on the substrate (solid lines) and particles on a 30 nm oxide spacer layer (dotted lines). Clear peaks in the Q_{scat} data can be seen, corresponding to the localized surface plasmon resonance. It is observed that the height of the Q_{scat} peak is doubled for the 150 nm diameter particle *directly* on the Si compared to the case where the oxide layer is present, in agreement with previous work.[10] Without the spacer layer the resonance is clearly redshifted from a wavelength of 675 nm to ~1200 nm. This is a consequence of the overlap of electromagnetic near-field of the particle with the high-index Si.[5] The same trends are observed for the 200 nm diameter particle, with resonance peaks at wavelengths of 818 nm and beyond 1200 nm, with and without the oxide layer, respectively. The narrow peak at 740 nm can be attributed to a quadrupole excitation in the 200 nm particle. F_{subs} converges to over 90% for particles *directly* on Si and is reduced over all wavelengths for particles on a 30 nm oxide spacer layer. This F_{subs} enhancement is due to increased coupling into modes inside the Si with reduced spacer layer thickness as the near field overlaps with the substrate.[5] The quadrupole peak, identified in the Q_{scat} data for the 200 nm diameter particle, is associated with a dip in F_{subs}, showing that higher order excitations do not contribute effectively to light trapping.[13] The increased Q_{scat} and F_{subs} calculated for nanoparticles *directly* on the Si surface supports the experimental findings that the EQE enhancement is larger without the spacer layer. Since not all scattered light is coupled into the Si, the addition of a detached BSR is able to further boost EQE enhancement by reflecting a portion of the transmitted light.

The experimental data shows nearly identical V_{oc} values for the cells with and without an oxide layer on the surface, demonstrating that the relatively high bulk recombination of poly-Si and the existence of the BSF make it unnecessary to use a surface-passivating layer. This finding is further supported by PC1D (computer programme, Ref. 14) modeling results. When the recombination velocity was adjusted from zero (perfectly passivated) to 10^7 cm/s (worst recombination possible), the modeled efficiency variation was less than 1% (e.g., from absolute 5.05% efficiency to 5%), i.e., practically negligible.

In summary, we achieved 29% short-circuit current enhancement for planar evaporated solid-phase-crystallized poly-Si thin-film solar cells on glass, due to light trapping provided by Ag nanoparticles formed *directly* onto the rear Si surface of the cells, i.e., without an oxide spacer layer. With the inclusion of a detached BSR the short-circuit current can be further increased to 38%. This result surpasses conventional light trapping techniques for this solar cell type. Hence silver nanoparticles fabricated with a simple and relatively inexpensive process can provide effective light trapping for thin-film solar cells.

The authors thank Yuguo Tao for the SEM images taken at the Electron Microscope Unit of The University of New South Wales. The Centre of Excellence for Advanced Silicon Photovoltaics and Photonics is supported under the Australian Research Council's Centres of Excellence Scheme.

[1] M. A. Green, Appl. Phys. A: Mater. Sci. Process. **96**, 153 (2009).
[2] O. Kunz, Z. Ouyang, S. Varlamov, and A. G. Aberle, Prog. Photovoltaics **17**, 567 (2009).
[3] T. Sontheimer, P. Dogan, C. Becker, S. Gall, B. Rech, U. Schubert, T. Young, S. Partlin, M. Keevers, and R. Egan, Proceedings of the 24th European Photovoltaic Solar Energy Conference, Hamburg, September 2009, p. 2478.
[4] M. Werner, U. Schubert, C. Hagendorf, J. Schneider, M. Keevers, and R. Egan, Proceedings of the 24th European Photovoltaic Solar Energy Conference, Hamburg, September 2009, p. 2482.
[5] K. R. Catchpole and A. Polman, Appl. Phys. Lett. **93**, 191113 (2008).
[6] S. Pillai, K. R. Catchpole, T. Trupke, and M. A. Green, J. Appl. Phys. **101**, 093105 (2007).
[7] M. Losurdo, M. M. Giangregorio, G. V. Bianco, A. Sacchetti, P. Capezzuto, and G. Bruno, Sol. Energy Mater. Sol. Cells **93**, 1749 (2009).
[8] P. Matheu, S. H. Lim, D. Derkacs, C. McPheeters, and E. T. Yu, Appl. Phys. Lett. **93**, 113108 (2008).
[9] F. J. Beck, A. Polman, and K. R. Catchpole, J. Appl. Phys. **105**, 114310 (2009).
[10] F. J. Beck, S. Mokkapati, A. Polman, and K. R. Catchpole, Appl. Phys. Lett. **96**, 033113 (2010).
[11] O. Berger, D. Inns, and A. G. Aberle, Sol. Energy Mater. Sol. Cells **91**, 1215 (2007).
[12] FDTD Solutions, www.lumerical.com
[13] C. Hägglund, M. Zach, G. Petersson, and B. Kasemo, Appl. Phys. Lett. **92**, 053110 (2008).
[14] D. A. Clugston and P. A. Basore, Conference Record of 26th IEEE Photovoltaic Specialists Conference, Anaheim, September 1997, p. 207.